RESEARCH ARTICLE

ScienceAsia 29 (2003): 355-364

Heat and Mass Transfer during Deep-Fat Frying of Frozen Composite Foods with Thermal Protein Denaturation as Quality Index

Chairath Tangduangdee,* Sakarindr Bhumiratana and Suvit Tia

Department of Chemical Engineering, King Mongkut's University of Technology Thonburi, Bangkok 10140, Thailand.

* Corresponding author: E-mail: chairath.tan@kmutt.ac.th

Received 12 May 2003
Accepted 29 Aug 2003

ABSTRACT: Heat and mass (moisture) transfer during deep-frying of frozen composite food was simultaneously modeled using the moving boundary concept. An explicit finite difference method was used to solve the proposed model. A model food composed of a chicken breast coated with batter at both ends was used to validate the predicted center temperature during frying at the specified oil temperatures. Thermal denaturation of actin was, in this study, chosen as the quality index of the meat-based product being fried, and its corresponding kinetic parameters were experimentally determined from the DSC data with the assumption of a single-step irreversible reaction. Good agreement between the predicted and observed results could be obtained when a 0.3 mm vapor gap between material layers was added to the proposed mathematical model. Sensitivity studies showed that the varying oil temperature of $\pm 10^{O}$C did not dramatically affect the center temperature profile of the product. Oppositely, the center temperature of the product was notably affected by the gap width in the order of 0.1 mm and the batter thickness in the order of 1 mm.

KEYWORDS: deep-fat frying, moving boundary, protein denaturation.

INTRODUCTION

Deep-fat frying is a cooking process, in which food is immersed in edible oil at a temperature above the boiling point of water contained in that food; the oil temperature may range from 130 to 200^{O}C, but is generally between 170 to 190^{O}C.[1] During frying, heat and moisture transfer is coupled as in the drying process. The decreased moisture content of the fried food with elevated temperature causes many chemical reactions, such as browning, gelatinization, denaturation, etc. Studies of the time-temperature relation of meat product using protein denaturation as a quality indicator indicate that collagen and actin are the two most important proteins responsible for the quality of meat texture. The best texture is obtained with maximum collagen and minimum actin denaturations.[2] The research on frying has been getting more attention recently, however, the information on the engineering aspects of the process is still very limited.[3]

During the frying process, there are four distinct stages: (1) heat-up period, (2) surface boiling period, (3) falling rate period, and (4) bubble end point. The first and the forth stages may be generalized as non-boiling phases, while the second and the third stages are boiling phases. Before evaporation of moisture occurs, the surface heat transfer coefficient is about 250-300 W/m^2 K, which then increases to 800-1000 W/m^2 K due to the considerable turbulence of water vapor bubbles.[1] Many researchers have proposed mathematical models to describe the frying process, which can be classified into two groups; firstly, the single phase model,[4-7] and secondly, the two phase (or moving boundary) model.[1,8-11] For the latter case, modeling of the moving boundary at the crust/core interface is needed. Yamsaengsung and Moreira[12,13] proposed the transport model for tortilla chip during frying and cooling processes, which also takes into account various structural changes, including shrinkage and expansion due to puffing. The studied parameters (water saturation, oil saturation and temperature) were simulated and were found to agree well with the experimental data. In addition, the effects of oil temperature and the product thickness on the oil content of the final product were studied and it was found that the higher frying temperature and the thicker product led to the lesser oil content of the product. Moreover, it was found that the cooling temperature nearest to the temperature of the fried product contributed to the least amount of oil absorption.

So far, most studies on frying have been performed

using unfrozen homogeneous materials rather than frozen composite products, which are normally available for the customer in a supermarket. From a food quality point of view, most research has also been limited to the magnitude of oil and moisture content in products. The objective of this research, therefore, is to improve and extend the mathematical model to enable its application to deep-fat frying of composite frozen foods using thermal protein denaturation as a quality index.

Govering Equations

To describe the heat and moisture transfer during deep-fat frying of frozen composite foods, the process is divided into two stages. The initial stage is called the heating-up period and is considered the same as the thawing process, in which there is no mass transfer. As soon as the surface temperature reaches the boiling point of water, the surface boiling stage starts, and crust portion begins to form and continuously grows (see Fig.1). The crust region is defined as a region that has negligible liquid water associated with it, and its temperature may exceed the boiling point of water and approach the frying oil temperature.[1] At this stage, the compositions of the food change due to moisture loss. Using published data,[9,20] some dimensionless groups of the process were studied. With 0.5 mm of crust thickness (s), the Biot number (hs/k_{cr}), defined as an internal thermal resistance of solid relative to an external thermal resistance, is 1.14, which is much greater than 0.1. This implies that the crust thickness is significant as a thermal barrier.[14] Another dimensionless group analyzed is the Stefan number ($C_{cr}(T_s - T_b)/\lambda$), which is defined as a ratio of the sensible heat to the heat released or absorbed for phase change at the crust/core interface. Its estimated value of 0.12 (<1.0) implies that sensible heat has a small influence on the phase-change process, and thus the heat transfer in the crust region could be simply described using the pseudo-steady state condition[15]. To formulate the mathematical model, the following assumptions were made:

(1) The composite food consists of a layer of one type of material and is coated at both ends by the other type of material with negligible heat and mass transfer resistance between the adjacent layers.

(2) Conduction is the main mechanism of heat transfer in the crust region, which means the crust is considered as a thermal barrier.

(3) Food compositions, such as moisture content, carbohydrate, protein, fat, fiber, and ash in each phase are in thermal equilibrium conditions.

(4) The energy required for chemical changes, such as heat of gelatinization or heat of denaturation, is small compared with the latent heat of phase change.

(5) A sharp moving boundary is assumed.

Heating-up Stage

Our own preliminary experiments showed that this period lasted about 20 to 80 seconds depending on the oil temperature. Heat transfers from the hot oil to the product via natural convection at the surface and conduction through the product.[1] Using the enthalpy balance, the heat transfer equation can be written as[16]:

$$\frac{\partial H^l}{\partial t} = \frac{\partial}{\partial x}\left[k^l\{T\}\frac{\partial T^l}{\partial x}\right] \qquad (1)$$

where H^l is the volumetric specific enthalpy (J/m^3), superscript l=I denotes the outer layer when $0 < x < x^I$, and l = II denotes the inner layer when $x^I < x < x^{II}$, $k^l\{T\}$ is the thermal conductivity (W/mK), which depends on the temperature of substances, T is the product temperature (^{O}C) and x is the distance in x-direction (m). Eq (1) is subjected to the following boundary and initial conditions:

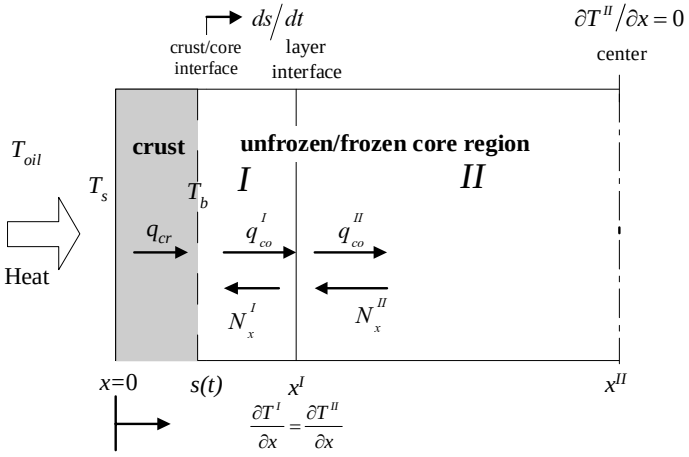

Fig 1. Heat and mass transfer through frozen composite materials.

$$k\frac{\partial T}{\partial x}\bigg|_{x=0} = h_0\left(T_{oil} - T_s(t)\right) \qquad \text{at } x = 0,\ t > 0 \tag{2a}$$

$$\frac{\partial T^I}{\partial x}\bigg|_{x=x^I} = \frac{\partial T^{II}}{\partial x}\bigg|_{x=x^{II}} \qquad \text{at } x = x^I,\ t > 0 \tag{2b}$$

$$\frac{\partial T^{II}}{\partial x} = 0 \qquad \text{at } x = x^{II},\ t > 0 \tag{2c}$$

$$T^I = T^{II} = T_0 \qquad \text{at } 0 < x \le x^{II},\ \text{t=0} \tag{2d}$$

where T_s is the temperature (^{O}C) at the product surface and varies with the frying time.

Heat Transfer Formulation in the Surface Boiling Stage

As soon as the surface temperature reaches to the boiling point, bubbles can be seen and the crust portion immediately forms. Under the pseudo-steady state assumption, the heat transfer in the crust region can be expressed by Laplace's equation given by:

$$\frac{\partial^2 T^I}{\partial x^2} = 0 \qquad \text{at } 0 < x \le s(t) \tag{3}$$

which is subjected to the following boundary conditions:

$$\frac{ds^I}{dt} = \frac{1}{\lambda m^I_{w0}}\left(q_{cr} - q^I_{co}\right) \qquad T^I(0,t) = T_s(t) \qquad \text{at } x = 0,\ t > 0 \tag{4a}$$

$$T^I(s,t) = T_b = \text{constant} \quad \text{at } x = s(t),\ t > 0 \tag{4b}$$

For the core region, heat convection due to moisture movement was added to Eq (1) when the temperature of each node in the core region reaches the melting point. Hence, the heat transfer equation can be written as

$$\frac{\partial H^I}{\partial t} = \frac{\partial}{\partial}\left[k^I\frac{\partial T^I}{\partial x}\right] + N^I_x C_{pw}\frac{\partial T^I}{\partial x} \qquad \text{at } s(t) < x \le x^{II} \tag{5}$$

and is subjected to the following boundary conditions:

$$T^I(s,t) = T_b \qquad \text{at } x = s(t),\ t > 0 \tag{6a}$$

$$k^I\frac{dT^I}{dx} = k^{II}\frac{dT^{II}}{dx} \qquad \text{at } x = x^I,\ t > 0 \tag{6b}$$

$$\frac{\partial T^{II}}{\partial x} = 0 \qquad \text{at } x = x^{II},\ t > 0 \tag{6c}$$

where N^I_x is the moisture flux (kg/m^2 s) and defined in Eq (16). An additional boundary condition is the location of the crust/core interface, $s(t)$, which is determined by making an energy balance over the crust/core interface during a time interval Δt:

(7a)

or written in an explicit finite difference form:

$$s^{j+1} = s^j + \frac{\Delta t}{\lambda m^I_{wo}}\left(q_{cr} - q^I_{co}\right) \tag{7b}$$

which is subjected to the initial condition:

$$s = 0 \qquad \text{at } t = 0 \tag{7c}$$

where is the initial moisture concentration (kg/m^3) of the outer layer, q_{cr} and q^I_{co} are the heat flux into and out of the interface, respectively.

$$q_{cr} = \frac{(T_{oil} - T_b)}{1/h + s(t)/k_{cr}} \quad \text{and} \quad q_{co} = \left(\frac{k_b + k_m}{2}\right)\frac{(T_b - T^j_m)}{\Delta x^j_n} \tag{8}$$

Subscripts *b* and *m* indicate the point where boiling occurs and the node point adjacent to the crust/core interface, respectively. Superscript *j* indicates the present time *j*, and Δx^j_n is the distance from the crust/core interface to the next node inside the core region as shown in Fig 2.

In addition, the surface temperature is determined by making an energy balance at the surface. After rearranging to avoid dividing by the crust thickness, the balance becomes[14]:

$$T_s(t) = \left[T_b + \left(s(t)hT_{oil}/k_{cr}\right)\right] \Big/ \left[1 + \left(s(t)h/k_{cr}\right)\right] \tag{9}$$

Heat Transfer at the Layer Interface

Referring to Eq (6b) when heat resistance between the adjacent layers is negligible, the temperature at the layer interface can be calculated by making an energy balance over the corresponding segment in the computational domain as illustrated in Fig 2:

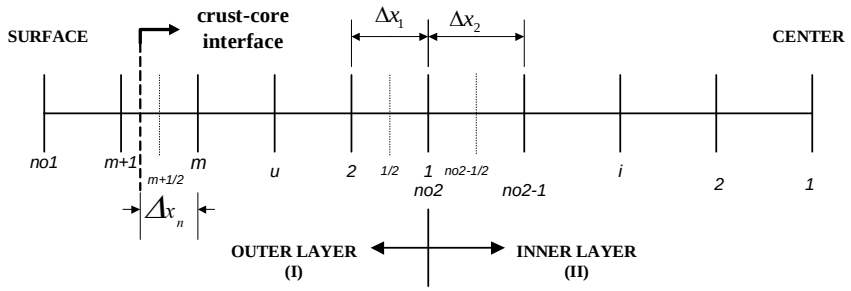

Fig 2. Node spacing and numbering of a composite material and the movement of the crust/core interface.

$$k^{I}_{1+1/2}\frac{\left(T^{I}_{2}-T^{I}_{1}\right)}{\Delta x_1}=k^{II}_{no2-1/2}\frac{\left(T^{II}_{no2}-T^{II}_{no2-1}\right)}{\Delta x_2} \quad (10)$$

where Δx_1 and are the grid distance for the outer and the inner layers, respectively. The thermal conductivity was determined at the half node spacing of each segment. Substituting for T^{II}_{no2}, the temperature at the interface can be calculated from the following equation:

$$T^{I}_{1}=\frac{\zeta_2 T^{I}_{2}+\zeta_1 T^{II}_{no2-1}}{(\zeta_1+\zeta_2)} \quad (11)$$

where: $\zeta_1=\frac{\Delta x_1}{k^{I}_{1+1/2}}$ and $\zeta_2=\frac{\Delta x_2}{k^{II}_{no2-1/2}}$ (12)

Modeling Moisture Transfer during the Surface Boiling Stage

Fick's second law of diffusion assuming a constant moisture diffusivity (D_m) was chosen to describe the moisture transfer within the frying product. Further, it is assumed that there is no mass resistance and there is equilibrium at the layer interface defined by an equilibrium distribution coefficient (k).[17] The change in concentration (m_d) of both layers can be expressed by:

$$\frac{\partial m^{l}_{d}}{\partial t}=D^{l}_{m}\frac{\partial^2 m^{l}_{d}}{\partial x^2} \quad (13)$$

which is subjected to the following boundary and initial conditions:

$$m^{I}_{d}(s,t)=0 \qquad \text{at } x=s(t),\ t>0 \quad (14a)$$

$$m^{I}_{d}=\kappa m^{II}_{d} \qquad \text{at } x=x^{I},\ t>0 \quad (14b)$$

$$\frac{\partial m^{II}_{d}}{\partial x}=0 \qquad \text{at } x=x^{II},\ t>0 \quad (14c)$$

$$m^{I}_{d}(x,0)=m^{I}_{d0} \text{ and } m^{II}_{d}(x,0)=m^{II}_{d0} \text{ at } t=0 \quad (14d)$$

Moisture in dry basis can be correlated to the moisture concentration (m_w) in kg water/m^3 by:

$$m_w=\rho\frac{m_d}{(1+m_d)} \quad (15)$$

where ρ is the density (kg/m^3) of the product and is dependent on the temperature and compositions, D^{l}_{m} is the effective moisture diffusion (m^2/s) of each layer (l=I for the outer layer and l=II for the inner layer). Thus, the mass flux of moisture (N_x in kg water/m^2 s) expressed in Eq (5) in each layer of the core region can be calculated by:

$$N^{l}_{x}=-D^{l}_{m}\frac{\partial m^{l}_{w}}{\partial x} \quad (16)$$

Protein Denaturation Kinetics

The denaturation kinetics of protein represented by actin is expressed by the general rate law of a single irreversible reaction:

$$\frac{d\mathrm{D}}{dt}=k_d(1-\mathrm{D})^n \quad (17)$$

which is subject to the initial condition:

$$\mathrm{D}(x,0)=0 \qquad \text{at } x^{I}<x\le x^{II},\ t=0 \quad (18)$$

Table 1. Input parameters for heat transfer validation and process simulation.

Food type	Property	Source
Batter	54% moisture, 40.08% carbohydrate, 3.24% protein, 0.39% fat, 1.78% fiber, 0.51% ash	Present study
	D_m=5.9x10^{-9} m^2/s	
	Ru^*=0.13, k_{cr}=0.05 W/m K, ,T_z=-1.0°C, 0% porosity	Farkas *et al* (1996)[21]Assumed
Chicken breast	76.07% moisture, 0% carbohydrate, 23.16% protein, 0.59% fat, 0% fiber, 0.18% ash	Present study
	Ru^*=0.22, D_m=2.0x10^{-8} m^2/s, T_z=-1.0°C, 0% porosity	Assumed
	Process conditions	
	Oil temperature: 160, 180 and 190°C	Specified
	Boiling temperature: 102°C	Farkas et al (1996)[21]
	Natural heat transfer coefficient (h_0): 250-300 W/m^2 K	"
	Average heat transfer coefficient (h): 500 W/m^2 K	"

The temperature dependence of the denaturation rate constant (k_d) could be described by the Arrhenius law:

$$k_d = Z \exp(-E/RT) \quad (19)$$

where D is the denatured protein fraction (dimensionless), n is the order of reaction, Z is the Arrhenius frequency factor (s^{-1}), E is an activation energy (J/mol), R is the universal gas constant (8.314 J/mol K), and T is an absolute temperature of sample (K). Eq (17) can be written in an explicit finite difference form as:

$$D_i^{j+1} = D_i^j + k_d\{T_i^j\}(1-D_i^j)^n \cdot \Delta t \quad (20)$$

where Δt is the time step (s), subscript i is i^{th} node and superscripts j and j+1 are the present time step j^{th} and new time step j^{th} +1, respectively.

Simulation of the Frying Process

The governing heat and moisture equations along with their initial and boundary conditions were solved using an explicit finite difference scheme. The computation for the product temperature requires the thermophysical properties as a function of temperature and food compositions. These properties, namely mass specific enthalpy (H), heat capacity (C_p), density (r), and thermal conductivity (k) were estimated for each kind of foods based on the ideal mixture concept.[18,19] Such properties were validated for frozen and unfrozen states and were found to favorably agree with experimental data from various sources. For the detailed explanation on the property formulation, the reader is referred to Tangduangdee.[11] To simulate the frying process, the properties were first programmed with MATLAB® as function files, which could be then recalled to convert the calculated enthalpy into temperature for a given time step at each node within the product. To ensure the computational stability, the stability criteria for heat transfer were examined at the core boundary and the center node. Since the heat transfer rate was relatively higher than that of mass transfer, the stability criteria for heat transfer were also used for the mass transfer calculation. Input parameters for the process simulation are shown in Table 1. To estimate the thermophysical properties of batter and chicken breast, their compositions were measured by AOAC standard method[18] for moisture, fiber, protein, and ash contents, while the remaining component of the product was assumed to be carbohydrate content. The ratio of unfreezable water content to solid content (Ru) needed in the property prediction was also assumed with reasonable accuracy, because its value falls within a narrow range for different classes of food products, i.e., 0.13 for bread and 0.22-0.27 for meat and fish muscle[17]. The use of an initial freezing temperature (T_z) of chicken breast of –1°C led to a good agreement between the temperature dependent specific heat and enthalpy obtained in the present study and the experimental data obtained from other sources[11]. From the preliminary experiments, the constant effective moisture diffusivity (D_m) of chicken breast was estimated[11]. Due to a vigorous turbulent phenomenon, an average heat transfer coefficient of 500 W/m^2 °C was used during the second stage of frying.

Materials and Methods

To validate the proposed heat transfer model, a deep fat fryer, which has a total volume of 29 liters, was built with the temperature controller of ± 1°C accuracy. Two stirrers running at 200-300 rpm were installed and a large volume (25 liters) of palm oil was used to ensure the uniformity of oil temperature during frying (see Fig 3).

Chicken breasts were purchased from a local supermarket and were stored at 0±1°C. A whole sample was cut using a die having an inside diameter of 95 mm and was then put in a circular Teflon mold having an inside diameter of 95 mm and a thickness of 20 mm. To maintain uniformity, the sample was then trimmed to the required thickness. A modified thermocouple probe (Type T of 2-mm diameter), used for the canning process establishment, was inserted into the sample through a threaded hole on the side of the mold and screwed in. Batter slurry was prepared from batter mix flour (Global Food, Ltd.) mixed with distilled water at the ratio of 1.0:0.9 (by weight) to obtain 54 percent moisture content (wb). A thin circular Teflon mold of 5 mm thickness was placed on the enclosed chicken breast and then filled with the batter. The batter was spread to acquire a uniform thickness prior to freezing for 2-3 hours. The other side of the sample was prepared in the same way. Afterwards, the whole sample was frozen overnight to lower its temperature to around –20°C before frying. Three replications at each frying oil temperature of 160, 180 and 190°C were conducted. During frying, the value of the center temperature of the sample was collected every 20 seconds using DataTaker model DT 605 with DeLogger Plus software. After frying, the fried sample was cut to measure the crust thickness using a Vernier Caliper (Mitutoyo: accuracy 0.05 mm.).

A Perkin Elmer model Pyris I Differential Scanning Calorimeter (DSC) was used to study the denaturation of protein in chicken breast meat. Following an ASTM standards (E 2041-99), a sample weight of 10-15 mg was weighed and loaded into an aluminum pan and

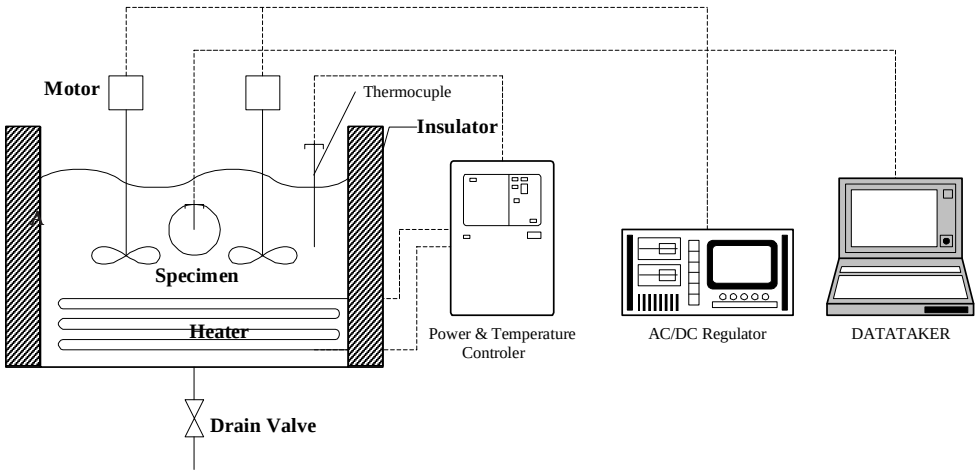

Fig 3. Schematic diagram of a deep-fat fryer with a control unit and data acquisition system.

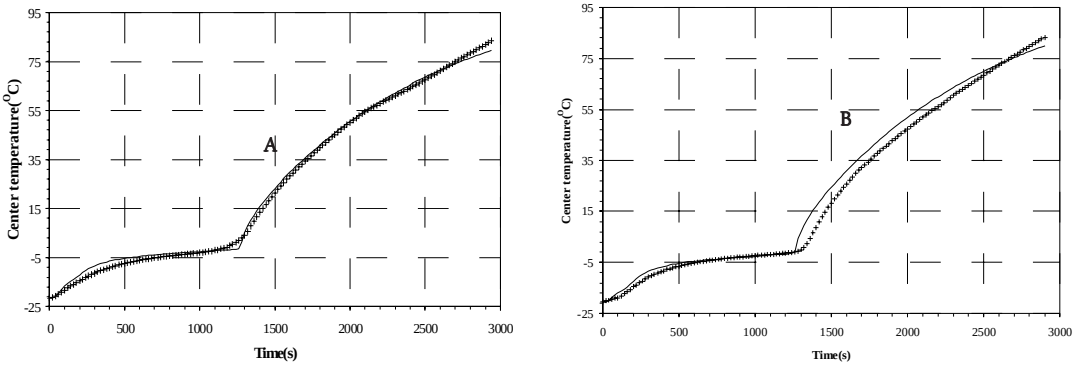

Fig 4. Comparison of the center temperature histories of a frozen battered chicken breast during frying between the predicted and experimental data (+) with 6 mm thickness of batter, 22 mm thickness of chicken meat and 0.3 mm of gap.
(A) Oil temperature: 160°C, initial sample temperature: -21.58°C
(B) Oil temperature: 180°C, initial sample temperature: -20.39°C

then hermetically sealed. The sample pan was placed into the apparatus and scanned from 40-100 °C at the heating rate of 10°C/min under ambient pressure using an empty aluminum pan as the reference. Ice mixed with water was used as the cooling medium. After cooling down to the ambient temperature, the enclosed sample was weighed again to check for leakage. The Borchardt and Daniels approach (ASTM E 2041-99) was applied to estimate the kinetic parameters from the thermal curve obtained from the DSC.

Results

Validation of the Heat Transfer Model

The proposed mathematical model was numerically solved and used to simulate the center temperature of frozen battered chicken breast and the crust thickness using the parameters given in Table 1. During the simulation, the thermophysical properties of batter depended only on temperature,[10] whereas those of chicken breast varied with compositions in addition to the product temperature. Although no gap was assumed at the beginning of this study, the actual gap of 0-3 mm wide was observed from the experiments. An average gap of 0.3 mm was, therefore, included in the model by extending Eq (11) to:

(21)

and $$T_{no2}^{II} = \frac{\zeta_2 T_2^I + (\zeta_1 + \zeta_3) T_{no2-1}^{II}}{(\zeta_1 + \zeta_2 + \zeta_3)} \quad (22)$$

where: $$\zeta_3 = \frac{\Delta x_g}{k_g} \quad (23)$$

Δx_g is the gap width (m) and k_g is the thermal conductivity of water vapor in the gap (W/m °C). In addition, the thickness values of 6 mm for batter and 22 mm for chicken breast were used for the simulation to take into account the sample expansion after freezing.

Fig 4 depicts the simulated and observed center temperature of frozen battered chicken breast during

Table 2. Linear regression analysis and final crust thickness at various oil temperatures.

Oil temperature(°C)	Linear regression parameter			Final crust thickness (mm)	
	R^2	Slope (m)	Intercept(b)	Observed	Predicted
160	0.998	0.99	1.27	1.80±0.25	1.60
180	0.994	1.00	2.22	2.20±0.28	2.00
190	0.998	0.95	-1.28	2.50±0.45	2.10

frying in oil at 160 and 180°C. The temperature at the center of the product started to increase within 20-30 seconds after immersing the product in the hot oil. As the temperature approached the freezing point of the product, it slightly increased due to the phase change of water. Once the phase change occurred completely, the temperature rose sharply. Good agreement between the observed and predicted results was noted with high correlation. The analyzed results were compared with the ideal fitting case; that is R^2 =1.0, slope (m)=1.0, and intercept (b)=0.0[11]. Linear regression analysis of the center temperature of the samples fried at different oil temperatures yielded the results shown in Table 2. Since the heat transfer coefficient was very high, heat transfer into the crust region was dominated by the thermal conductivity of the crust and the temperature difference between that of hot oil and the product surface (see Eq 8). A favorable agreement between the observed and predicted final crust thickness at various oil temperatures was obtained when the crust thermal conductivity of 0.05 W/m.K is used. However, the crust formation mechanism is very complicated because not only moisture loss occurs but its structure also changes. These changes affect the transport parameters and heat transfer mechanism. The crust formation mechanism indeed merits study in the future.

Fig 5 shows the influences of oil temperature, batter thickness and gap width on the center temperature of the product. The simulation showed that the thickness of batter and the gap width had a crucial influence on the product temperature profiles and the time of phase change, which were only slightly affected by the oil temperature. However, the oil temperature significantly affected the final crust thickness (see Table 2).

DSC Thermogram and Simulation of Protein Denaturation

Study of thermal protein denaturation of a whole chicken breast showed three major endothermic transition temperatures at 62.87, 76.62, and 83.24°C (Fig 6). These transitions were attributed to the denaturation of myosin, collagen and actin, respectively. The transition temperatures agreed with the published results, which are given at 62, 70, and 82 °C, respectively.[22] Based on the Borchardt and Daniels kinetics, the parameters of actin protein denaturation were 1.29±0.12 for n, 866.7±87 kJ/mol for the activation energy, and 128±30 min^{-1} for log Z at 95% confidence level. Once the temperature of the product was known, the amount of denatured actin could be calculated.

Fig 7 presents the simulated denaturation of actin at the layer interface and at the center of the composite product being fried at the various oil temperatures. It is obvious that the rate of denaturation was not dependent on the oil temperature but on the starting and end points of denaturation. Because protein denaturation occurred very rapidly and could not be stopped at any frying time, verification of the kinetics model was difficult. However, according to the USDA (A-A-20150) regulation for safe consumption of poultry products, the core temperature of product must reach 83°C, i.e., the minimum amount of denatured actin should be 50 percent (see Fig 7).

Conclusion

A mathematical model of the simultaneous heat and moisture transfer of a frozen composite food during deep-fat frying is presented in this paper. Using the moving boundary concept and the enthalpy formulation, the proposed model was found to successfully predict the temperature profiles of the frying product. From the sensitivity studies, it was found that the thickness of the batter, in the order of 1 mm, and gap between food layers, in the order of 0.1 mm, had a crucial influence on the temperature profiles. On the contrary, the variation of oil temperature within ± 10°C did not significantly affect the center temperature of the product; oil temperature may be varied within ± 10°C without significantly affect the center temperature of the product. This means that special attention must be paid to the product thickness and the adhesion between sample layers during the preparation step, otherwise error will result. However, the high temperature of the frying oil (≥190°C) tends to darken the product color. In order

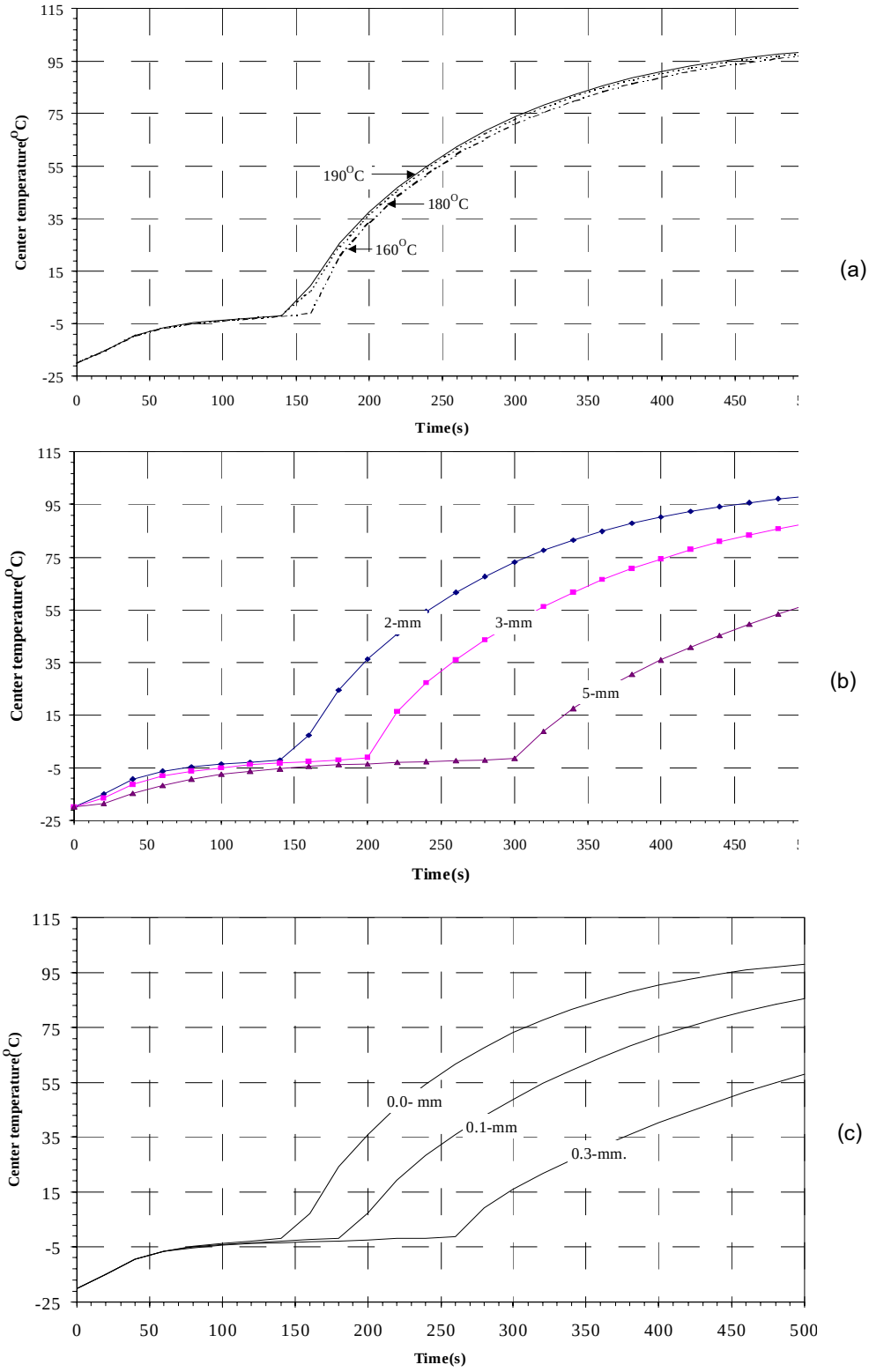

Fig 5. Simulation of the influences of oil temperature, batter thickness and gap width on the predicted center temperature of a frozen battered chicken breast with 10-mm thickness of chicken meat. Initial sample temperature: -20°C
(a) Impact of oil temperature with constant batter thickness: 2 mm and no gap
(b) Impact of batter thickness with constant oil temperature: 180°C and no gap
(c) Impact of gap width with constant batter thickness: 2 mm and oil temperature: 180°C.

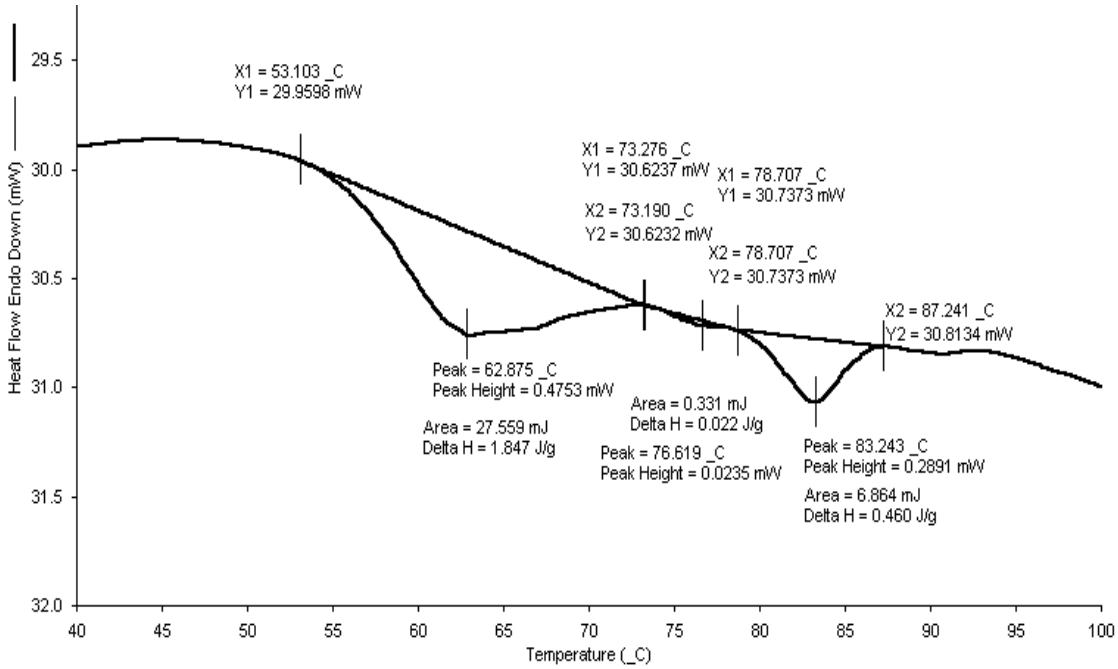

Fig 6. DSC thermal curve of a whole chicken breast muscle. Sample weight: 14.920 mg. Heating rate: 10°C.

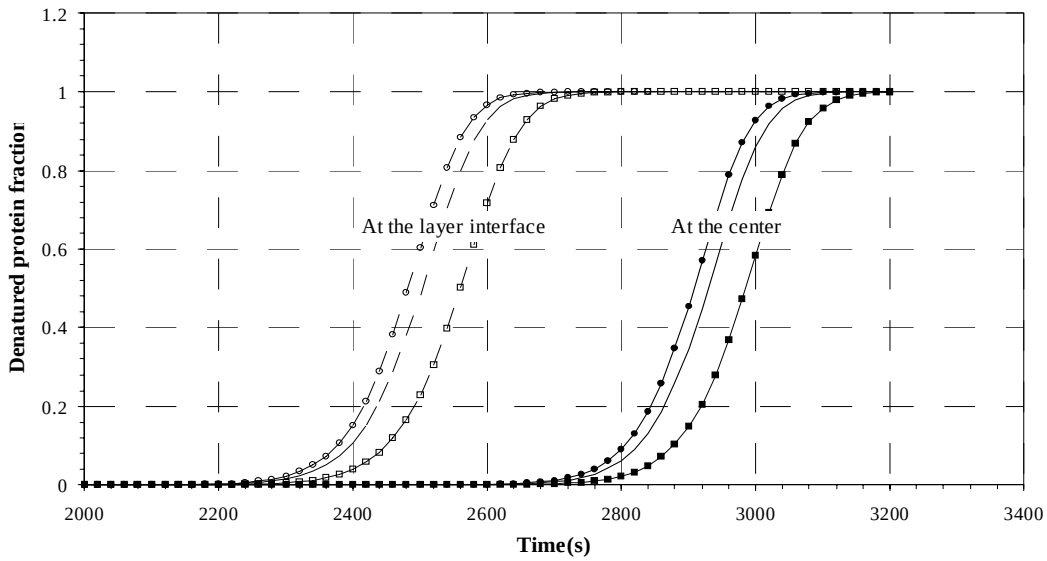

Fig 7. Denaturation of actin protein at the layer interface and at the center of product obtained from the mathematical model during frying at various oil temperatures. Frozen food model: 22 mm thickness of chicken breast coated with 6 mm thickness of batter and assumed 0.3 mm of gap.
—□—, —■— for 160°C of oil temperature with initial temperature of –21.58°C,
——, —— for 180°C of oil temperature with initial temperature of –20.39°C,
—o—, —•— for 190°C of oil temperature with initial temperature of –21.28°C.

to maximize the eating quality of deep fried poultry products, the actin denaturation at the center of the product should be about 50 percent in order to satisfy the requirement of the USDA (core temperature ≥83°C). Nevertheless, this criterion may not be suitable for a thin sample due to the narrow range of protein transition. The transport processes with the moving boundary proposed herein is useful for further studies on other quality indices of the product.

ACKNOWLEDGEMENTS

The authors gratefully acknowledge the National Science and Technology Development Agency of

Thailand (NSTDA) for supporting this research work financially. We are also grateful to Dr. Sakamon Devahastin (Food Engineering Department, King Mongkut's University of Technology Thonburi, Thailand) for his help during the preparation of this manuscript.

REFERENCES

1. Farkas BE, Singh RP and Rumsey TR (1996) Modeling heat and mass transfer in immersion frying, I. Model development. *J Food Engineering* **29**, 211-226.
2. Tennigen A and Olstad S (1979) Computer controlled heating of meat with respect to protein denaturation. In: *Food Process Engineering*, Vol.1, Food Processing Systems, (Edited by Linko P, Mälkki Y, Olkku J and Larinkari J), pp. 146-151. Applied Science Publishers, London.
3. Singh RP (1995) Heat and mass transfer in foods during deep fat frying. *J Food Technology* **49**, 134-137.
4. Mittelman N, Mizrahi Sh and Beek Z (1984) Heat and mass transfer in frying. In: *Engineering and Food*, Vol. 1, Engineering science in food industry, (Edited by McKenna B), pp. 109-116, Elsevier, London.
5. Moreira, RG, Palau J and Sun X (1995) Simultaneous heat and mass transfer during the deep fat frying of tortilla chips. *J Food Process Engineering* **18**, 307-320.
6. Ngadi MO, Watts KC and Correia LR (1997) Finite element method modeling of moisture transfer in chicken drum during deep fat frying. *J Food Engineering* **32**, 11-20.
7. Roa MVN and Delaney RAM (1995) An engineering perspective on deep fat frying of breaded chicken pieces. *Food Technology* **49**, 138-141.
8. Farid MM and Chen XD (1998) The analysis of heat and mass transfer during frying of food using a moving boundary solution procedure. *Heat and Mass Transfer* **34**, 69-76.
9. Vijayan J (1996) *Heat transfer during immersion frying of frozen foods*, PhD dissertation, University of California, Davis.
10. Vijayan J and Singh RP (1997) Heat transfer during immersion frying of frozen foods. *J Food Engineering* **34**, 293-314.
11. Tangduangdee C (2002) *Heat and mass transfer during deep fat frying of frozen composite food with thermal protein denaturation as a quality index*. PhD thesis, King Mongkut's University of Technology Thonburi, Bangkok, Thailand.
12. Yamsaengsung R and Moreira RG (2002) Modeling the transport phenomena and structural changes during deep fat frying, Part I: model development. *J Food Engineering* **53**, 1-10.
13. Yamsaengsung R and Moreira RG (2002) Modeling the transport phenomena and structural changes during deep fat frying, Part II: model solution & validation. *J Food Engineering* **53**, 11-25.
14. Özi°ik MN (1993) *Heat conduction*, 2nd ed. Wiley, New York.
15. Lock GSH (1994) Latent heat transfer: An introduction to fundamentals. pp 81-94. Oxford University Press, New York.
16. Mannapperuma JD and Singh RP (1988) Prediction of freezing and thawing times of foods using a numerical method based on enthalpy formulation. *J Food Science* **53**, 626-630.
17. Geankoplis, CJ (1972) *Mass transport phenomena*. pp 239-242. Holt, Rinehart and Winston, USA.
18. Choi Y and Okos MR (1986) Effect of temperature and composition on the thermal properties of foods. In: *Food Engineering and Process Applications,* Vol.1, (Edited by Maguer ML and Jelen P) pp 93-101. Elsevier Applied Science Publishers, New York.
19. Mannapperuma JD and Singh RP (1989) A computer-aided method for the prediction of properties and freezing/thawing times of foods. *J Food Engineering* **9**, 275-304.
20. AOAC International (1995) *Official Methods of Analysis of AOAC International*. 16th ed. p. 44. 1. 05. AOAC International, Virginia.
21. Farkas BE, Singh RP and Rumsey TR (1996) Modeling heat and mass transfer in immersion frying, II. Model solution and verification. *J Food Engineering* **29**, 227-248.
22. Bircan C and Barringer SA (2002) Determination of protein denaturation of muscle foods using the dielectric properties. *J Food Science* **67**, 202-205.